A Small Signal Capacitance Model for A Metallic Electrochemical Electrode in the Charge Transfer Region

A.R.M. Alamoud

Electrical Engineering Department College of Engineering, King Saud University
P.O. Box 800, Riyadh 11421, Saudi Arabia

In this paper a small signal capacitance model for an electrochemical electrode is developed. This model takes into consideration the conventional Helmholtz layer and diffusion layer capacitances in addition to the capacitance of a homogeneous middle layer between the two previous layers. The small signal capacitance calculated by this model increases with the electrode potential reaching a maximum at certain specific voltage and then decreases in qualitative agreement with the measured C-V curve. By quantitative comparison of the theoretical and experimental C-V curves satisfactory agreement was found at the lower potentials. At the higher potentials where the reaction rate is appreciable the measured capacitance is smaller than the theoretical one. This is attributed to the formation of gas bubbles leading to a continuous decrease of electrode area with increased reaction rate.

Introduction

One of the most common techniques to characterize the transition regions formed between two different materials in contact is the determination of the relationship between the small signal capacitance of a metallic cathode and the potential drop across these transition regions. It is found that the measured small signal capacitance of a metallic cathode evolving hydrogen increases with the cathode potential reaching maximum value after which it decreases rapidly to small values [1,2]. It is observed that the rapid decrease in the capacitance occurs at the same time of formation of large macroscopic gas bubbles at the electrode surface. This C-V behaviour is not yet rigorously modeled. The objective of this paper is to derive relationships relating the small signal capacitance to the electrode potential based on a physical model taking into consideration the maximum cation solubility in the electrolyte and the formation of gas bubbles on the electrode surface. The theoretical and experimental results will be compared to verify the model.

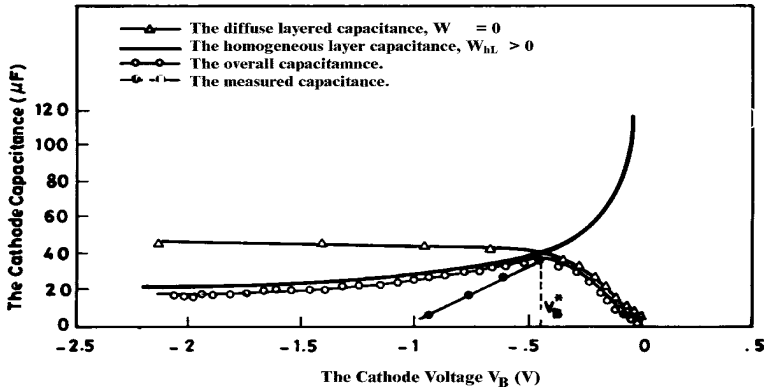

Fig. (1) Charge distribution in an electrochemical cathode.

1. The Space Charge Distribution

Assume the cation distribution shown in Fig.1 where a negative voltage V is applied on the electrode. If the applied voltage is sufficiently high, the concentration of the hydrogen ions in the first Outer Helmholtz Plane (OHP) exceeds the maximum solubility owing to the self interaction between the positively charged hydrogen ions and the absence of their negative neutralizing charges because of the depletion of the anions from the surface of the cathode. Increasing the voltage further a second OHP forms and so on. This means an outer Helmholtz layer will be built as shown in Fig.1. Since there is thermal random motion of the ions, their concentration can not change abruptly from N_h (the concentration in the Helmholtz layer) to that value in the bulk N_b. There will be a diffusion gradient towards the bulk and a diffused layer will be formed.

Because of the hydration sheath around the positive hydrogen ion they cannot get closer to the cathode surface than the first outer Helmholtz plane. This layer will be filled by nearly fully oriented water dipoles.

According to this distribution there are now four different layers in the electrolyte facing the cathode surface. They are the water dipole layer, the Helmholtz homogeneous positive layer, the diffused layer and the homogeneous bulk of the electrolyte.

Let us assume that in the diffused layer the excess ion concentration $N_d(x)$ decays exponentially with position,

$$N_d(x) = N_h(e^{-(x-x_d)/L} - 1) \quad \text{for } x \geq x_d \tag{1}$$

where L is a certain characteristic length. Perhaps a more suitable distribution is that resulting from the assumption of quasi-equilibrium. This means that the drift and diffusion currents balance out. It follows in this case that [3]:

$$N_d(x) = N_b(e^{-[V(x)-V(\infty)]/V_T} - 1) \tag{2}$$

where $V(\infty)$ is the potential at the bulk of the electrolyte, $V(x)$ is the potential at any point x, $V_T = kT/q$ is the thermal equivalent voltage and N_b is the background concentration.

The electric field distribution can be determined using the Poisson's equation, i.e.

$$\frac{\partial E}{\partial x} = \frac{\rho}{\varepsilon} \tag{3}$$

where ρ is the excess ion charges in the interface region (see Fig. 1) and ε is the dielectric constant.

Outside regions 1, 2 and 3 the electric field is zero because there is no excess charges. Assuming that the potential at $(x = \infty)$ is zero such that $V(x)$ will be measured relative to $V(\infty)$.

2. The Electric Field E(x)

In region 3, Eqn.(3) becomes:

$$\frac{\partial E_3}{\partial x} = \frac{q N_b}{\varepsilon_3}(e^{-V(x)/V_T} - 1) \tag{4}$$

Multiplying the left hand side of Eqn.(4) by $\left(\frac{V_T}{V_T}\right)$ ($\partial V/\partial V$), rearranging and integrating, one gets

$$E_3^2 = \frac{2q\,N_b\,V_T}{\varepsilon_3}\left(e^{-V(x)/V_T} + \frac{V(x)}{V_T} - 1\right) \qquad (5)$$

The electric field at the edge of the diffused layer $E_3(x)$ can be found in terms of the voltage drop on the diffused layer at $x = x_d$, i.e. $V_d(x_d)$.

$$E_3(x_d) = [\frac{2q\,N_b\,V_T}{\varepsilon_3}]^{1/2}[\,\frac{V_d}{V_T} + (e^{-V_d/V_T} - 1)\,]^{1/2} \qquad (6)$$

The voltage V_d can be found in terms of N_h as at $x = x_d$, $N_d(x_d) = N_h$ can be substituted in Eqn. (2), then

$$N_h = N_b\,(e^{-V_d/V_T} - 1) \text{ or } -V_d = V_T\,\ell n\,(\frac{N_h}{N_b} + 1) \qquad (7)$$

In region 2 the Poisson's equation has the form

$$\frac{\partial E_2}{\partial x} = \frac{q\,N_h}{\varepsilon_2} \qquad (8)$$

Integrating, the electric field is found to be

$$E_2 = \frac{-q\,N_h}{\varepsilon_2}(x_d - x) + \frac{\varepsilon_3\,E_3}{\varepsilon_2} \qquad (9)$$

As there is no free charge in region 1 adjacent to the cathode surface, the electric field E_1 will be constant and because of electric flux continuity we have,

$$\varepsilon_1 E_1 = \varepsilon_2 E_2(x_h) \qquad (10)$$

Substituting Eqn. (10) into Eqn. (9) it follows that

$$E_1 = \frac{-q\,N_h}{\varepsilon_1}(x_d - x_h) + \frac{\varepsilon_3\,E_3}{\varepsilon_1} \qquad (11)$$

3. The Potential Distribution V(x)

The potential V(x) at any point x can be obtained by integrating the electric field from ∞ to x,

$$V(x) = \int_{\infty}^{x} dV = -\int_{\infty}^{x} E\,dx \qquad (12)$$

The electric field distribution is schematically shown in Fig.2, where it is assumed that $\varepsilon_1 < \varepsilon_2 < \varepsilon_3$ as the electric field $E_1 < E_2 < E_3$ and the orientation of the water dipoles increases as x decreases. This distribution corresponds to Eqns. (6), (9) and (11).

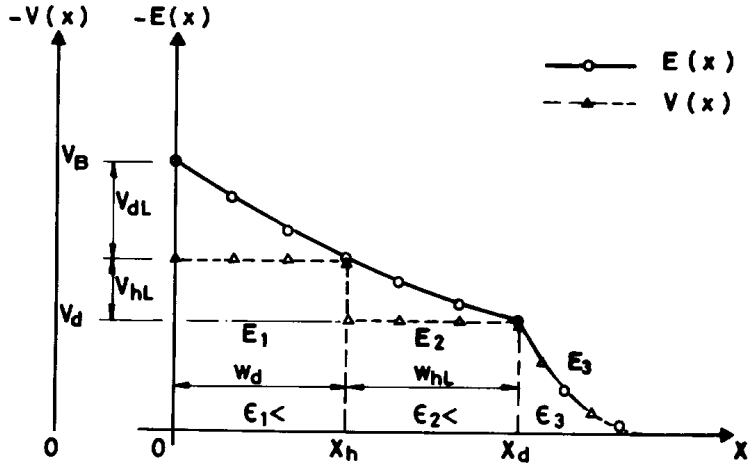

Fig. (2) Electric field and the potential distributions.

Based on Eqn.(12) and the electric field distribution, the potential distribution V(x) takes the form shown in Fig. 2, where the total potential difference V_B is distributed across the three layers, i.e.

$$V_B = V_d + V_{hL} + V_{dL} \tag{13}$$

where V_d, V_{hL}, and V_{dL} are the potential differences across the diffused layer, the Helmholtz layer and the dipole layer respectively[4]. These voltages are related to the area under the (E-x)-curve as follows:

$$V_d = -\int_{\infty}^{X_d} E_3(x)dx \tag{14a}$$

$$V_{hL} = -\int_{x_d}^{x_h} E_2(x)\,dx \tag{14b}$$

and

$$V_{dL} = -\int_{x_h}^{o} E_1(x)\,dx \tag{14c}$$

The potential drop, across the Helmholtz layer, V_{hL} can be obtained by substituting Eqn.(9) into Eqn.(14b) and integrating, i.e.

$$V_{hL} = \frac{-q N_h}{\varepsilon_2} W_{hL}^2 + \frac{\varepsilon_3 E_3}{\varepsilon_2} W_{hL} \qquad (15)$$

Here V_{hL} is intentionally expressed in terms of Helmholtz layer width, W_{hL}, which varies with V_{hL} while the other quantities in Eqn.(15) are fixed. Substituting Eqn.(11) into Eqn.(14c) and integrating we obtain

$$V_{dL} = \left(\frac{-q N_h x_h}{\varepsilon_1}\right) W_{hL} + \left(\frac{\varepsilon_3 E_3 x_h}{\varepsilon_1}\right) \qquad (16)$$

According to this equation as V_{dL} increases W_{hL}, increases linearly, while the other quantities remain unchanged.

The total cation charge Q^+ (C/cm^2) is the sum of the charges in the diffused layer Q^+_d and the charges in the Helmholtz layer Q^+_{hL}, i.e.

$$Q^+ = q N_h W_{hL} + \varepsilon_3 E_3 (x_d) \qquad (17)$$

4. The Small Signal Capacitance C

Now the small signal capacitance for an electrochemical cathode can be derived. By definition,

$$C = \frac{\partial Q^+}{\partial V_B} = \left(\frac{\partial Q^+}{\partial W_{hL}} \Big/ \frac{\partial V_B}{\partial W_{hL}}\right) \qquad (18)$$

Combining Eqns. (18), (17), (16), (15), and (13) one gets

$$\frac{1}{C} = \frac{1}{(\varepsilon_1 / x_h)} + \frac{1}{(\varepsilon_2 / 2 W_{hL})} + \frac{1}{\varepsilon_2 / \left\{\frac{2\varepsilon_3 V_T}{q N_h}\left[1 - \frac{N_b}{N_h}\ell n\left(1 + \frac{N_h}{N_b}\right)\right]\right\}^{1/2}} \qquad (19)$$

or $$1/C = 1/C_1 + 1/C_2 + 1/C_3 \qquad (19a)$$

In order to see how the capacitance C changes with the voltage V_B, let us express W_{hL} in terms of V_B. Combining Eqns. (13), (15), (16), (7) and (6) one gets

$$a_v W_{hL}^2 + b_v W_{hL} + (c_V + V_B) = 0 \qquad (20)$$

where $$a_v = \frac{q N_h}{\varepsilon_2}, \qquad (20a)$$

$$b_v = \frac{q\,N_h\,x_h}{\varepsilon_1} + \frac{\sqrt{2q\,\varepsilon_3\,N_h\,V_T}}{\varepsilon_2}\left[1 - \frac{N_b}{N_h}\,\ell_n\left(1+\frac{N_h}{N_b}\right)\right]^{1/2} \qquad (20b)$$

and

$$c_v = V_T\,\ell_n\left(1+\frac{N_h}{N_b}\right) + \frac{x_h\sqrt{2q\,\varepsilon_3\,N_h\,V_T}}{\varepsilon_2}\left[1 - \frac{N_b}{N_h}\,\ell_n\left(1+\frac{N_h}{N_b}\right)\right]^{1/2} \qquad (20c)$$

Equation (20) can be solved to obtain the width of the Helmholtz layer, W_{hL}, i.e.,

$$W_{hL} = \frac{-b_v \pm \sqrt{b_v^2 - 4a_v(c_v + V_B)}}{2a_v} \qquad (21)$$

The positive solution is the only physically allowed solution in this case.

Since V_B is negative, therefore as it increases, W_{hL} increases and from Eqn. (19b), C_2 decreases with the square root of the applied voltage. This is really an important result showing that the overall capacitance C decreases by increasing the applied voltage above the voltage V_B^* at which $W_{hL} = 0$. According to Eqn. (19)

$$-V_B^* = c_v \qquad (22)$$

At this voltage, C_2 tends to increase to infinity and the overall capacitance C becomes C^* such that the capacitance C^* will be the maximum overall capacitance, i.e.

$$\frac{1}{C^*} = \frac{1}{C_1} + \frac{1}{C_3} \qquad (23)$$

5. The Capacitance C for $|V_B| < |V^*_B|$

All previously derived relations for the electric field, potential and charges are valid for the voltage range $|V_B| < |V^*_B|$ except one has to set $W_{hL}=0$. Now the main parameter is the concentration of the cations at the first outer Helmholtz layer N_h. As V_B increases, N_h increases according to Eqn. (20c).

An expression for the capacitance in this voltage range can be derived from Eqn. (17),

$$V_B = \frac{\varepsilon_3\,x_h}{\varepsilon_1}\,E_3 + V_d \qquad (24)$$

Differentiating Eqn. (24) with respect to E_3 and dividing the result by ε_3 yields

$$\frac{1}{C} = \frac{1}{(\varepsilon_1 / x_h)} + \frac{1}{\varepsilon_3 \dfrac{\partial E_3(x_d)}{\partial V_d}} \qquad (25)$$

Combining Eqns. (6) and (25) one gets

$$\frac{1}{C} = \frac{1}{\varepsilon_1 / x_h} + \frac{1}{\varepsilon_3 [\dfrac{qN_b}{2\varepsilon_3 V_T}]^{1/2} (e^{-V_d/V_T} - 1)[e^{-V_d/V_T} - 1 + \dfrac{V_d}{V_T}]^{-1/2}} \qquad (26)$$

It can be seen from this equation that the capacitance C for $|V_B| \leq |V_B^*|$ increases by increasing the voltage drop across the diffused layer V_d and hence by increasing V_B. One can eliminate E_3 by substituting Eqn. (6) into Eqn. (24). It follows that

$$V_B = \frac{\varepsilon_3 x_h}{\varepsilon_1} [(\frac{2qN_b V_T}{\varepsilon_3})(e^{-V_d/V_T} - 1 + \frac{V_d}{V_T})]^{1/2} + V_d \qquad (27)$$

One can calculate C as a function of V_B from Eqns. (26) and (27).

6. The Effect of the Anions on the Small Signal Capacitance

In the previous analysis it is assumed that the anion concentration is homogeneous and equal to the bulk concentration of the cations. For relatively large V_B values the effect of the anion is negligible but at small V_B values, their real distribution must be considered.

Fig. 3 shows the distribution of the anions and cations schematically in the front of a cathode for $|V_B| < |V_B^*|$. The negative charges on the cathode surface repel the anions away from the interface region. The excess ion charges in the interface region ρ is given by [3],

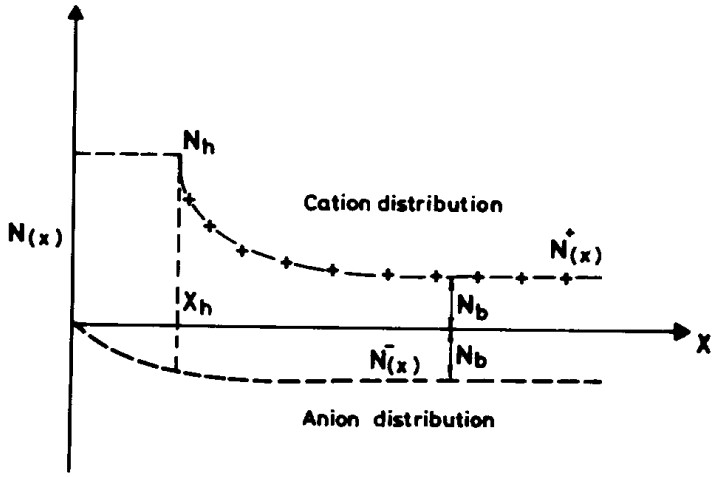

Fig. (3) The anion and cation distribution in the front side of a cathode.

$$\rho = -2q\, N_b \sinh (V(x)/V_T)$$

Substituting the above equation into Eqn. (3) gives the Poisson's equation

$$\frac{\partial E_3}{\partial x} = \frac{-2qN_b}{\varepsilon_3} \sinh\left[\frac{V(x)}{V_T}\right] \qquad (28)$$

Multiplying Eqn.(28) by $\left(\frac{V_T}{V_T}\right)(\partial V/\partial V)$ and integrating with the b.c. $V(\infty) = 0 = E_3(\infty)$ one gets,

$$E_3^2 = \left(\frac{4q\, N_b\, V_T}{\varepsilon_3}\right)\left(\cosh \frac{V(x)}{V_T} - 1\right) \qquad (29)$$

In region 1 at small V_B values the quantity of anions remaining in the dipole layers are appreciable and must be taken into consideration. The Poisson's equation in region 1 becomes

$$\frac{\partial E_1}{\partial x} = \frac{-qN^-}{\varepsilon_1} = \frac{-qN_b}{\varepsilon_1} e^{V(x)/V_T} \qquad (30)$$

This equation can be solved to get the net electric field at the metal surface with $V(x) = V_B$ at $x=0$, i.e.

$$E_1(o) = -\left[\frac{2q\, N_b\, V_T}{\varepsilon_1}\left(e^{V_B/V_T} - e^{V_d/V_T}\right) + \frac{\varepsilon_3^2}{\varepsilon_1^2}\left(\frac{4qN_b\, V_T}{\varepsilon_3}\right)\left(\cosh\frac{V_d}{V_T} - 1\right)\right]^{1/2} \qquad (31)$$

The total charge on the electrode is given by $Q = \varepsilon_1 E_1(0)$. In order to determine the capacitance one has to express V_B in terms of V_d,

$$V_B = -\int_{x_h}^{o} E_1 \, dx + V_d \qquad (32)$$

Eqn. (32) requires numerical solution. For a suitable solution, let us assume that the anions in the dipole layer are also negligible. Then the capacitance follows Eqn. (25) with the condition that $\partial E_3(x_d)/\partial V_d$ must be recalculated from Eqn. (29). Hence:

$$\frac{1}{C} = \frac{1}{(\varepsilon_1 / x_h)} + \frac{1}{\varepsilon_3 (\frac{2qN_b}{\varepsilon_3 V_T})^{1/2} (\cosh \frac{V_d}{V_T} - 1)^{1/2} + \sinh \frac{V_d}{V_T}} \qquad (33)$$

The value of the diffused layer capacitance at $V_d = 0$ is equal to the denominator of the second term in Eqn. (33) at $V_d = 0$,

$$C_3(o) = \varepsilon_3 / L_{db} \qquad (34)$$

where $L_{db} = (\varepsilon_3 V_T / 2qN_b)^{1/2}$ is the debye length in the bulk of the electrolyte.

It is interesting to notice that $C_3(o)$ is the minimum diffused layer capacitance at which the overall capacitance C will also be minimum. Increasing V_B, V_d also increases, C_3 increases and consequently C. For the voltage range where $C_3 >> C_1$, C_1 dominates the overall capacitance C which becomes insensitive to the voltage variation. For voltages $V_B > V_B^*$ a Helmholtz layer begins to appear and the overall capacitance begins to decrease again. The overall potential difference V_B can be obtained by substituting Eqn. (29) into Eqn. (24) at $V(x) = V_d$, i.e.

$$V_B = V_d - \frac{\varepsilon_3 x_h}{\varepsilon_1} [\frac{4qN_b V_T}{\varepsilon_3} (\cos h \frac{V_d}{V_T} - 1)]^{1/2} \qquad (35)$$

Eqns. (33), (35), (20), (21) and (18) can be used to calculate C as a function of the overall voltage V_B. The physical parameters concerning the cation concentrations N_b and N_h, the dielectric constants ε_1, ε_2, ε_3, the dimension x_h of the dipole layer and the temperature must all be known.

If the water dipole radius is r_w and the cation radius is r_i then it can be proved that:

$$x_h = (2 + \sqrt{3})\, r_w + r_i \qquad (36)$$

The maximum solubility of H^+ ions in water corresponding to the molecular arrangement is such that each ion is surrounded by six water dipoles forming a hexagonal cell. If the interionic distance $r_I = 4r_w + 2r_i$, then the number of H^+ ions/cm^3 is simply the inverse of the volume per ion v_i. This concentration is labeled previously by N_h,

$$N_h = \frac{1}{36\, r_w^3 \,(1 + \frac{r_i}{2\, r_w})^3} \qquad (37)$$

With the density of water being 3 gm/cm^3 and a molecular weight of 18, one can calculate the density of water molecules/cm^3, N_w. It is found that $N_w = 3.5 \times 10^{22}$ cm^{-3}. Assuming that the water molecules are spheres, the radius of the water molecule amounts to $r_w = 1.896 \times 10^{-8}$ cm. It should be noted that the ionic radius of the hydrogen ion $r_i = 0.529 \times 10^{-8}$ cm according to the first Bohr radius. Substituting the above values into Eqns. (36) and (37), one gets $x_h = 7.6 \times 10^{-8}$ cm (7.6 Å) and $N_h = 2.75 \times 10^{21}$ cm^{-3}, respectively.

For the following typical cathode parameters: $N_b = 6.3 \times 10^{18}$ cm^{-3}, $N_w = 3.5 \times 10^{20}$ cm^{-3}, $r_w = 1.896 \times 10^{-8}$ cm, $r_i = 0.529 \times 10^{-8}$ cm, $N_h = 2.75 \times 10^{21}$ cm^{-3}, and $x_h = 7.6 \times 10^{-8}$ cm together with the expressions of the cathode capacitance, as a function of the cathode voltage, and using Excel, the small signal capacitance of the cathode was calculated. The results are plotted in Fig. 4. It is clear from Fig. 4 that the diffused layer capacitance increases with the (negative) cathode voltage saturating at $|V_B^*| \geq 0.4$V while the homogeneous layer capacitance decreases. The overall capacitance of the cathode increases firstly with the cathode voltage V_B, reaching maximum value at $|V_B^*| > 0.4$V and then decreases following the homogeneous layer capacitance. It was found that as N_b increases the value of the capacitance at zero voltage increases and the maximum capacitance decreases. The voltage $|V_B^*|$ also increases. It must be mentioned here that these theoretical results agree with those measured for the dependence of the small signal capacitance on the electrode voltage as shown in Fig.4 in the lower voltage range. In the higher voltage range, the rate of decrease of C with V is smaller for the theoretical model. This may be attributed to capacitance-decreasing factors not taken into consideration in this model. The formation of gas bubbles which act as an insulator between the electrolyte and the metallic electrode is responsible for this discrepancy.

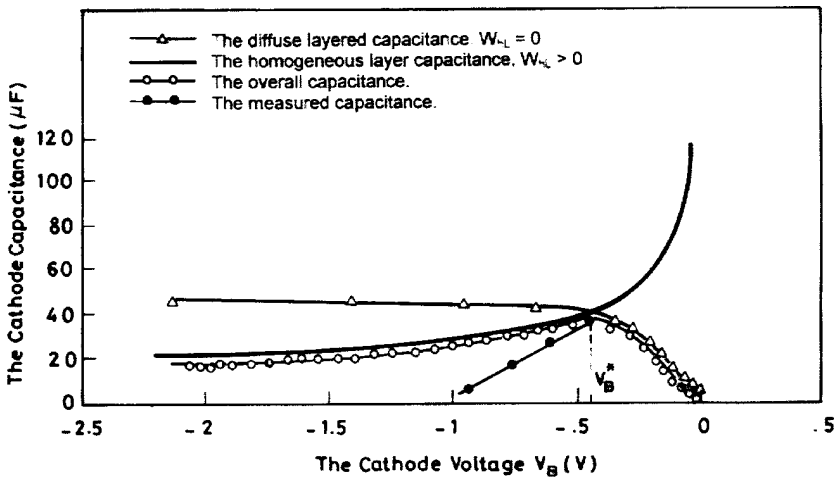

Fig. (4) The cathode capacitance as a function of the cathode voltage V_B for N_b = 3×10^{18} cm^{-3}.

7. Effect of Gas Bubbles on the Electrode Capacitance

Assume that the bubbles are statistically distributed at the cathode surface such that one can allocate a circular area with a radius r_b producing gas which is collected by a gas bubble in the center of the circular area and having a radius r. If the flux of hydrogen is ϕ and the density of the gas in the bubble is N, then one can write the rate equation.

$$N\, 2\Pi r^2\, dr = \phi\Pi\, (r_b^2 - r^2)\, dt, \ldots. \qquad (38)$$

where the gas evolved at the active area in a time dt with a flux ϕ, increases the radius of the gas collecting bubble by dr.

Normally the bubble grows from zero radius to a steady state radius r_{bf}, smaller than r_b, in a growth time T, hence

$$T = \int_0^{r_{bf}} \frac{2(N/\phi) r_b (r/r_b)^2 \frac{dr}{r_b}}{1 - \left(\frac{r}{r_b}\right)^2}, \qquad (39)$$

Now, one can express, the gas flux with bubble $\bar{\phi}$ in terms of the ratio (r_{bf}/r_b) as

$$\bar{\phi} = \frac{V_b N}{T \Pi r_b^2} \qquad (40)$$

where V_b is the volume of the bubble. Substituting Eqn. (39) into Eqn. (40) one gets,

$$\bar{\phi} / \phi = (r_{bf} / r_b)^3 / 3\gamma \qquad (41)$$

The ratio of $\bar{\phi}/\phi$ is at the same time the ratio of the effective area A_{ef} to the total area A,

$$\bar{\phi}/\phi = A_{ef} / A \qquad (42)$$

From Eqns. (39-42), the values of (A_{ef}/A) were calculated as a function of (r_{bf}/r_b) and the results are plotted in Fig. 5. We can see from this figure that the reaction rate remains almost unchanged for $r_{bf} < 0.3\ r_b$, after which it decreases rapidly, with r_{bf}/r_b, reaching very small fractions of the reaction rate without bubbles when (r_{bf}/r_b) approaches one. These results are very important and can have a great impact on the electrode design [5]. One has to design the electrode such that the bubbles cover no more than 9% of the total cathode area. On the other hand, it is observed experimentally that as the cathode current increases the bubble size increases which means that the active cathode area decreases and consequently the junction capacitance. In order to take the bubbles effect into consideration, one has to multiply all the previous expressions of the capacitances by the area factor (A_{ef}/A). From Fig. 4, at cathode voltage of 0.9V, the ratio of the measured to the theoretical capacitance is equal to about 0.2 which results in $(r_{bf}/r_b) = 0.97$ according to Fig. 5. This means that the cathode area is almost covered with bubbles that is an experimentally observable fact.

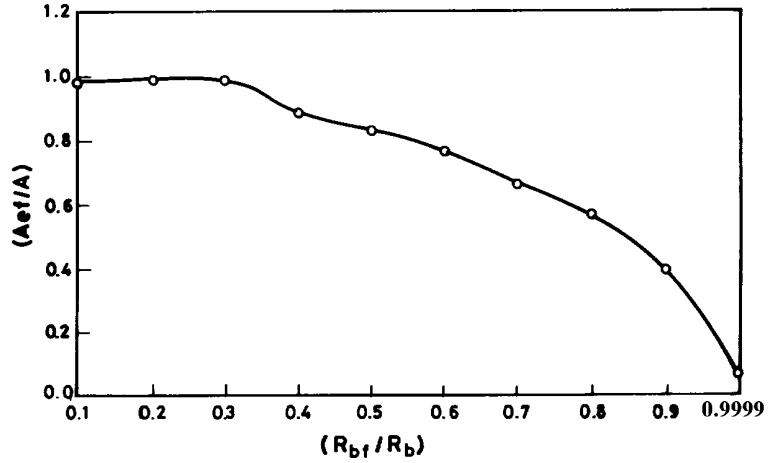

Fig. (5) The ratio of the active area A_{ef} to the total cathode area A as a function of the ratio of bubble radius to the radius of the available area per bubble.

For quantitative analysis of the capacitance, it is necessary to either measure (r_{bf}/r_b) as a function of the electrode voltage or develop a corresponding theoretical relationship. However, it is obvious now, that the formation of gas bubbles can drastically decrease the measured junction capacitance and can account for the observed C-V behavior since the decrease in the capacitance is coupled with a rise in the current value [2].

Conclusions

Because of the maximum solubility of the cation in the electrolyte, a middle layer with constant cation concentration will be formed between the Helmholtz layer and the diffused layer at relatively high cathode potential. The width of this middle layer increases with the potential and hence, its small signal capacitance decreases with the electrode potential.

The homogeneous middle layer with the maximum cation solubility is not sufficient to account for the rapid decrease of the measured C-V values. By taking the effect of the gas bubbles into consideration one could correctly explain the rapid fall in the C-V curve. One should not assume specific adsorbed species at the surface of the cathode. Further confirmation of this model may be achieved by the small signal capacitance variation with the frequency.

References

1. J.O'M Bockris and A.K.N. Reddy, Modern Electrochemistry, Vol. 2, Plenum Press, New York, 1993.

2. Alamoud, A.R.M., et al., "Hysolar Fundamental Research Program", Progress report # 3, Hysolar research group, COE, KSU, submitted to King Abdulaziz City for Science and Technology (KACST), Riyadh, Saudi Arabia, 1992.

3. Alamoud, A.R.M., et al., "Hysolar Fundamental Research Program", Progress report # 4, Hysolar research group, COE, KSU, submitted to King Abdulaziz City for Science and Technology (KACST), Riyadh, Saudi Arabia, April 1995.

4. Alamoud, A.R.M. and Zekry, A.A., "Static and small signal characterization of silicon photoelectrochemical cathodes for hydrogen production", Egyptian Journal of Solids, The Egyptian Society of Solid State Science and Applications, Vol. 17, No. 2, Cairo, Egypt, 1995.

5. Alamoud, A.R.M. and Zekry, Abdel Halim, "Basic Structures of Photoelectrochemical Cathodes for Hydrogen Production by Water Analysis", Sci. Bull. Fac. Eng. Ain Shams Univ., Vol. 32, No. 4, Cairo, Egypt, Dec. 31, 1997.